provide needed information. For each path the coordinates of antenna locations are accurately known; path profiles have been carefully read from detailed topographic maps and used to determine the required parameters for each path. A report on these paths and the long-term variability of transmission loss is in preparation.

Cumulative distributions of parameters for each group of paths are shown in table 7. In each group a range of frequencies from 40 to nearly 10,000 MHz, terrain types from smooth to mountainous, and a wide range of path lengths are represented. For the line-of-sight paths distributions of effective antenna heights are also shown, as this parameter is particularly important for these paths.

Values of basic transmission loss were calculated for each path using the methods described by Rice et al.(1967) and the computer methods described by Longley and Rice (1968). In each case these calculated values were compared with the long-term median value of basic transmission loss derived from measurements. Figures 54 through 57 show cumulative distributions of basic transmission loss, observed and predicted by both of these methods, and their differences ΔL.

Figure 54 shows that for known line-of-sight paths the earlier method calculates values that are too small by as much as 13 dB at the median, while the later "computer method" agrees well at the median but overestimates the loss by a wide margin for many of these paths. Several possible modifications of the methods were considered. Of these the best agreement with data was obtained by calculating the attenuation below free space A_{cs} as a function of the terrain parameter Δh, frequency f, effective antenna heights $h_{e1,2}$, and path length d. This attenuation is added to the free space loss to give calculated values of basic transmission loss:

$$L_{bc} = L_{bf} + A_{cs} \quad \text{dB} , \tag{3a}$$

Table 7. Cumulative Distributions of Path Parameters, for Established Communication Links

Parameter	Percentage									
	Min	10	20	30	40	50	60	70	80	90
	84 line-of-sight paths									
f	40	76	100	187	210	516	952	1310	4650	6825
d	11.9	18.6	27.5	42.7	69.0	80.5	100	113	125	143
Δh	2	18	22	46	56	88	126	191	302	454
h_{e1}	3.9	18.3	48.3	70.0	210	342	599	831	985	1021
h_{e2}	1.5	5.8	13.1	25.1	38	41	50	67	124	286
min. of $h_{e1,2}$	1.5	5.8	12.2	18.3	19	38	41	47	63	86
	46 one-horizon diffraction paths									
f	53	60	90	160	190	230	570	1000	2860	7270
d	10.4	50.9	76.0	76.4	98	101	113	122	128	195
Δh	29	73	76	84	89	90	93	114	160	415
	83 two-horizon diffraction paths									
f	41	60	92	98	101	160	190	210	492	1046
d	22	75	80	94	118	126	138	152	184	228
Δh	2	5	46	73	96	102	116	126	135	285
	340 scatter paths									
f	42	65	92	97	107	190	400	580	950	2100
d	76	150	195	205	225	265	295	335	365	480
Δh	4	22	38	65	95	105	135	175	250	345

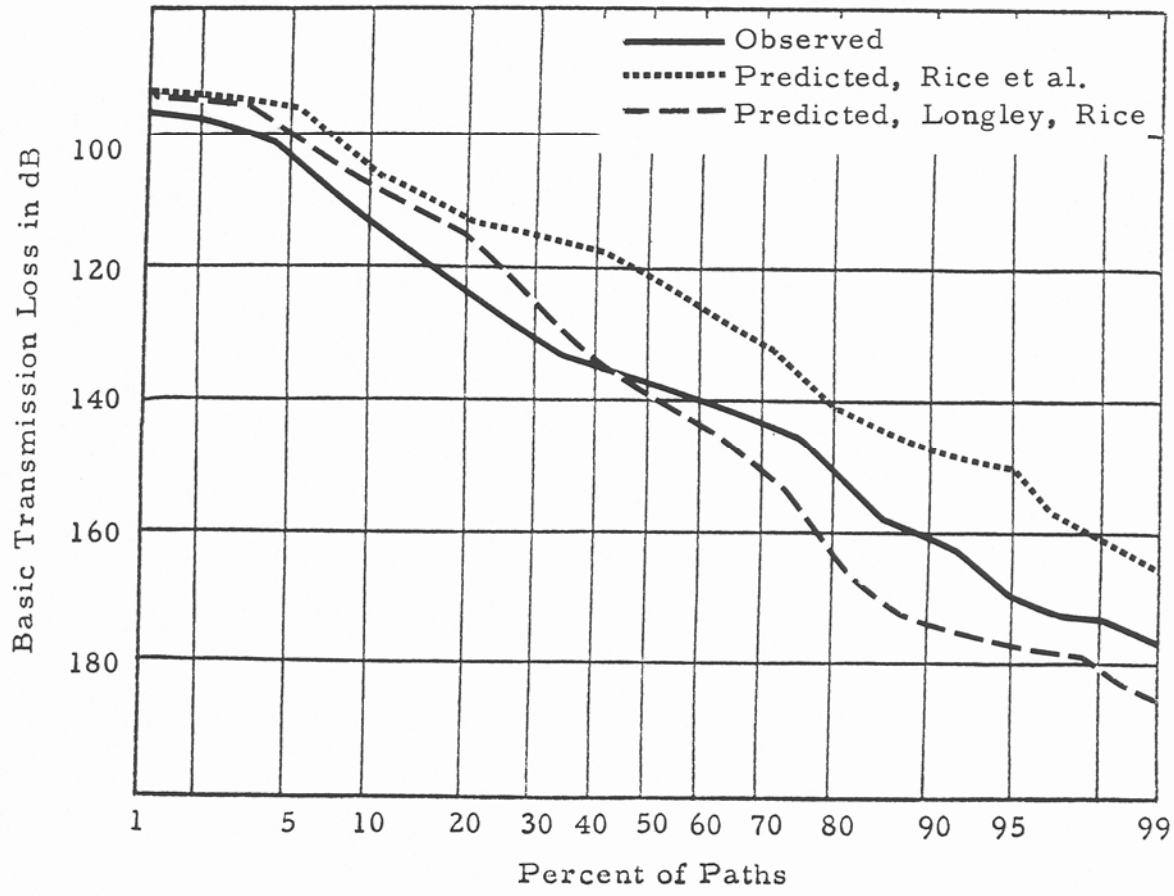

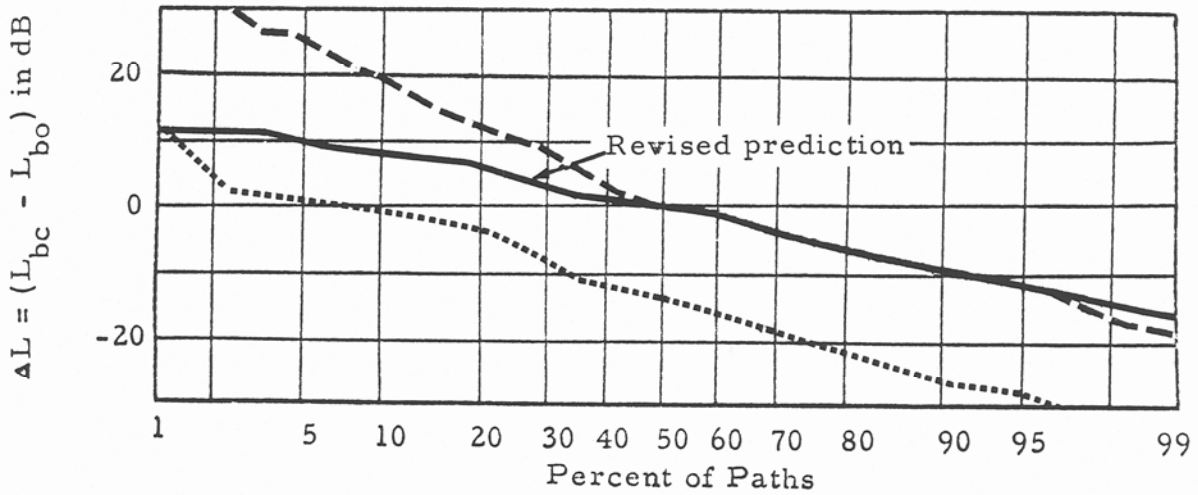

Figure 54. Cumulative distributions of basic transmission loss, observed and predicted, and of ΔL for 84 established line-of-sight paths.

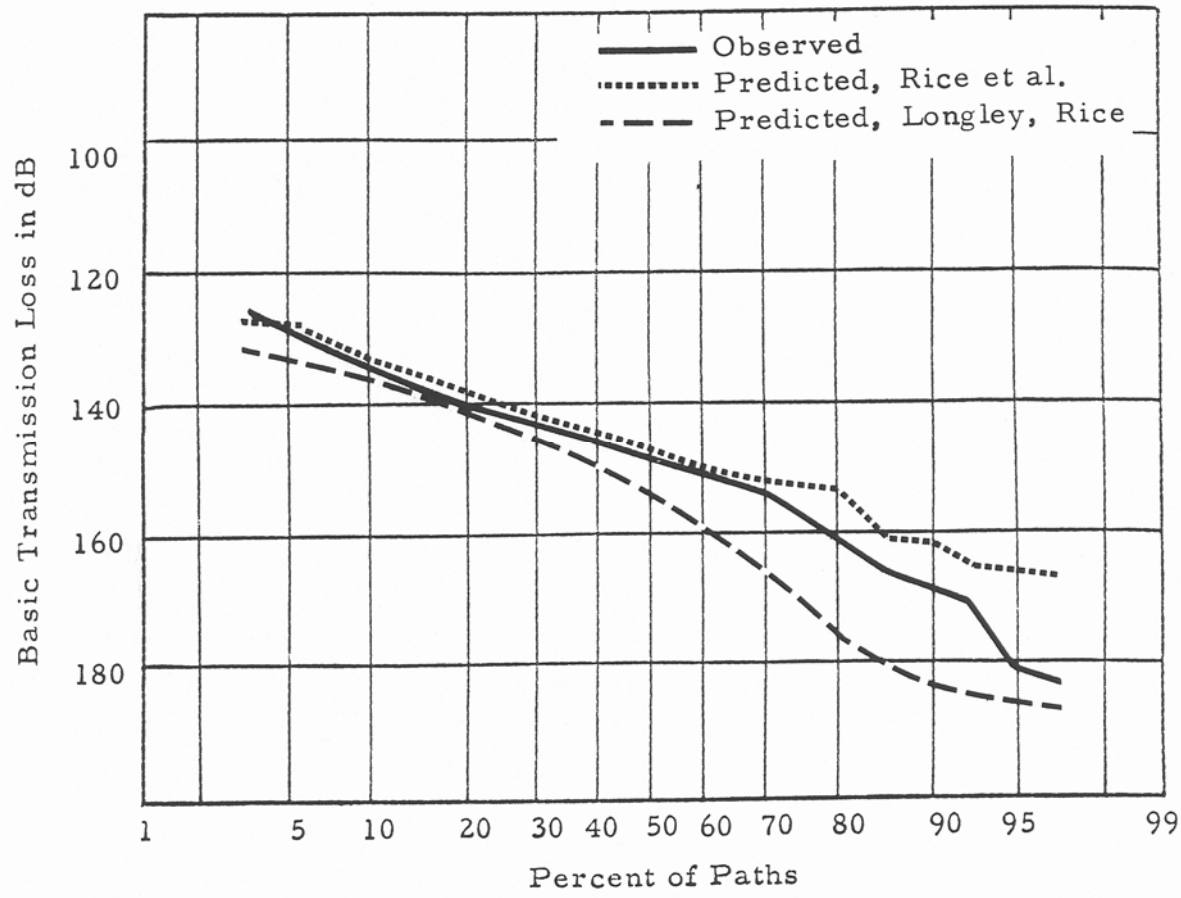

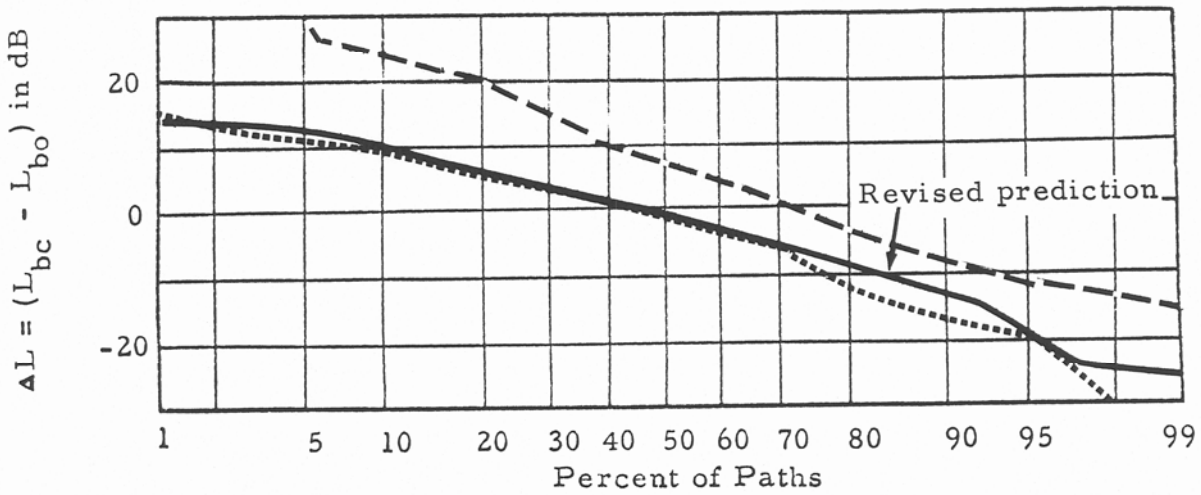

Figure 55. Cumulative distributions of basic transmission loss, observed and predicted, and of ΔL for 46 established one-horizon diffraction paths.

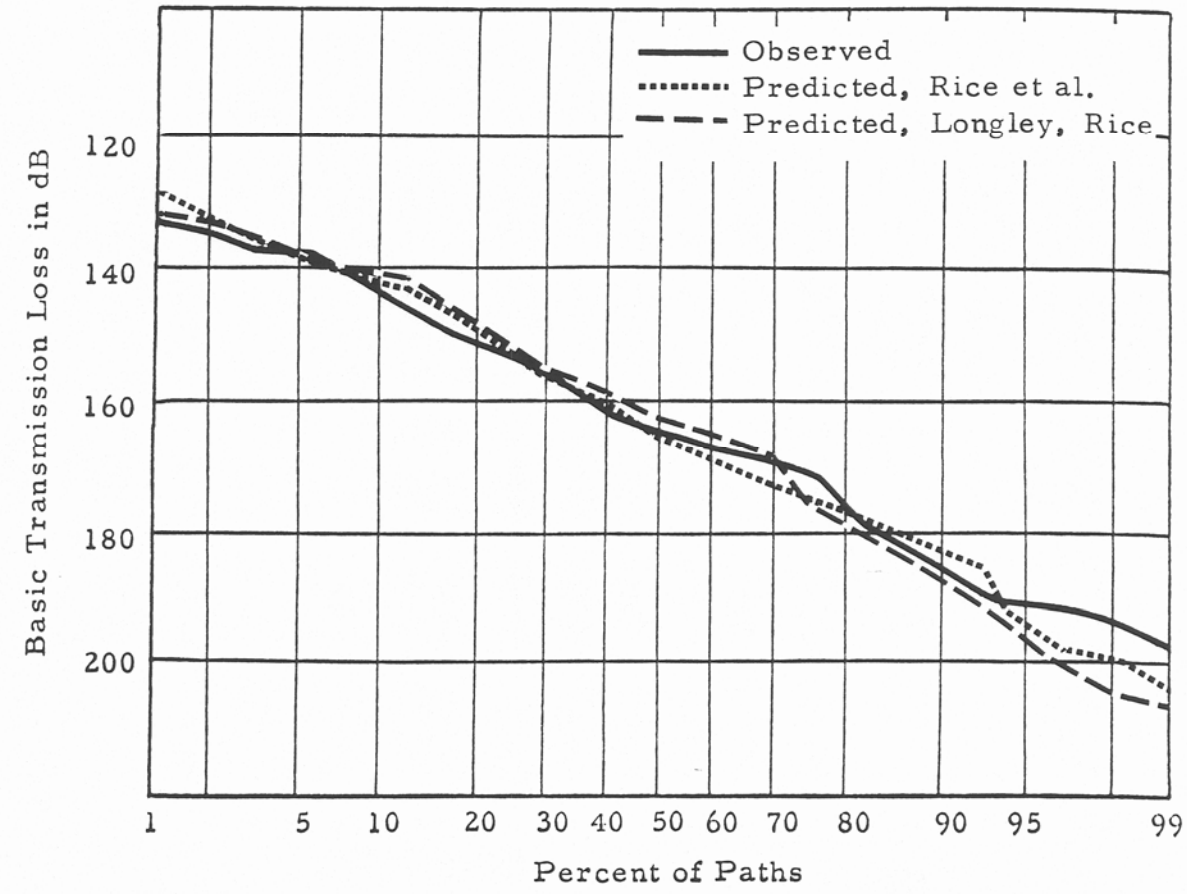

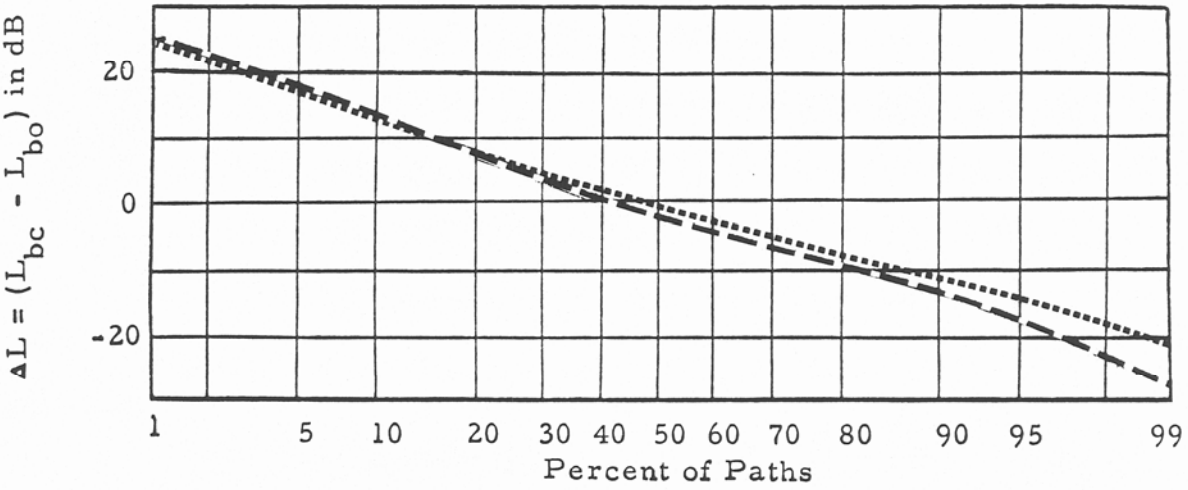

Figure 56. Cumulative distributions of basic transmission loss, observed and predicted, and of ΔL for 83 established two-horizon diffraction paths.

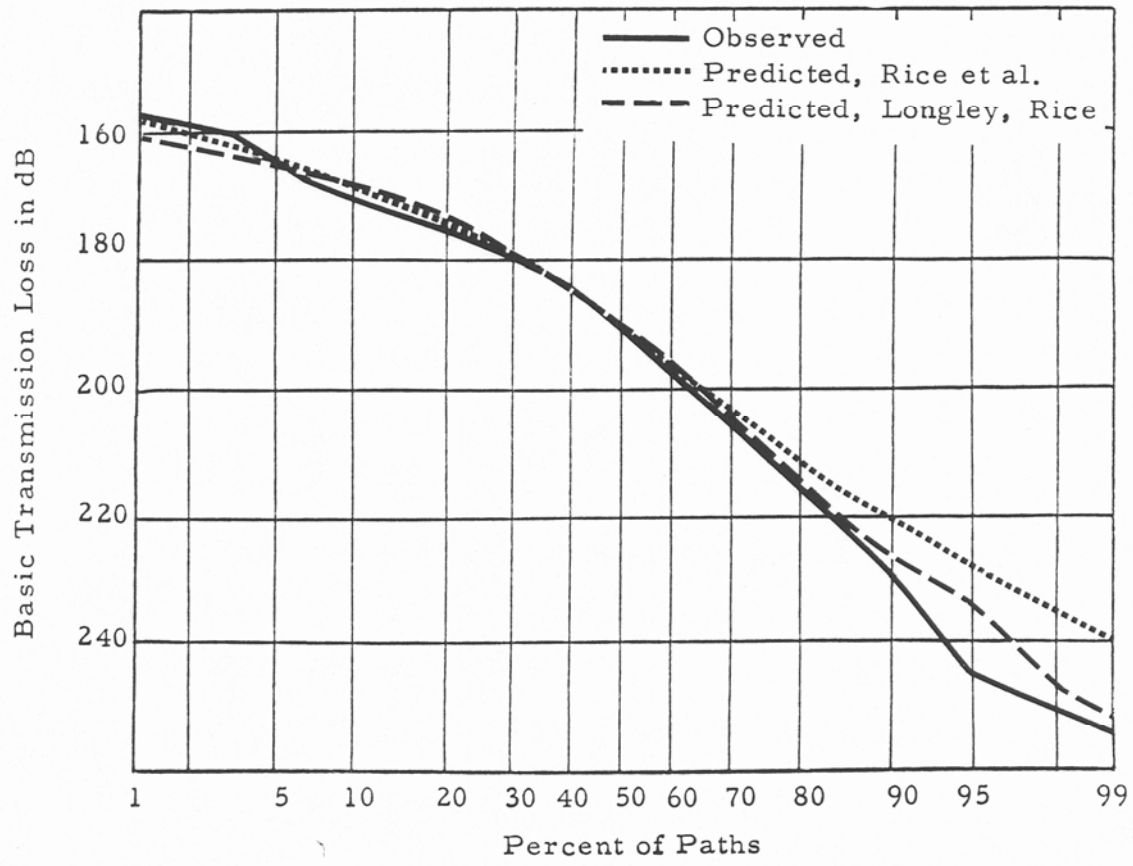

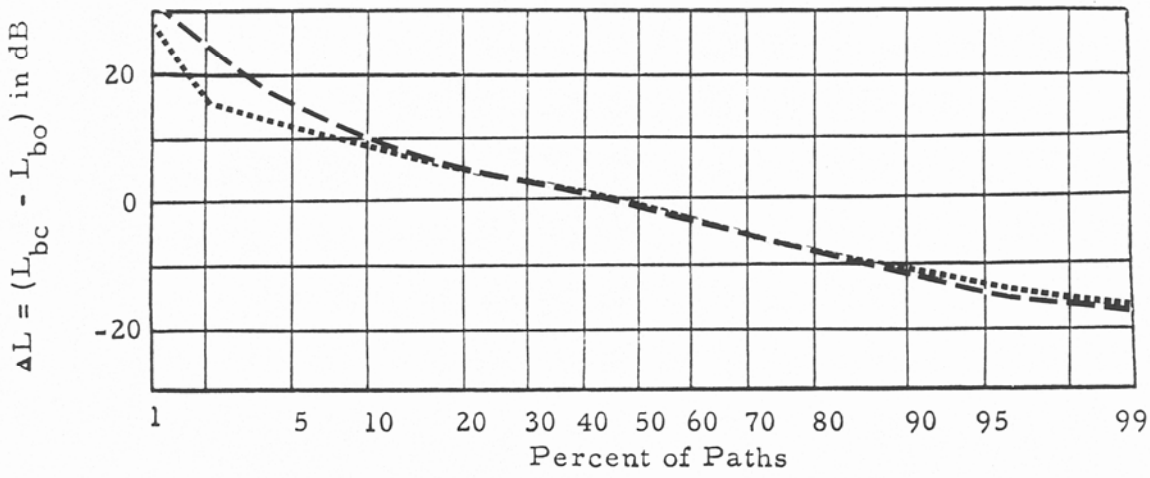

Figure 57. Cumulative distributions of basic transmission loss, observed and predicted, and of ΔL for 340 established forward scatter paths.

$$L_{bf} = 32.45 + 20 \log_{10} f + 20 \log_{10} d \quad dB, \tag{3b}$$

$$A_{cs} = 9 \left[1 + \exp(-0.01 \Delta h)\right] - 3.5 \log_{10} (\min h_{e1,2}/\lambda) + 0.07 d \quad dB. \tag{3c}$$

In these equations f is in MHz, d in km, with Δh, $h_{e1,2}$, and λ in m. This "revised prediction" gives excellent agreement with measured values for these 84 line-of-sight paths. Values calculated using this method will be compared with line-of-sight paths in the various data groups previously discussed.

Figure 55 shows calculated and observed values and their differences for 46 single-horizon paths. For some paths in this group the single horizon is an isolated mountain peak or ridge, while for others it is the surface of the sea or the bulge of the earth's surface. For most of these paths the earlier methods of Rice et al. (1967) give good results, but the computer method of Longley and Rice (1968) predicts too much attenuation. In this case also several modifications of the computer method were tested. The best comparison with data is obtained using Fresnell-Kirchoff knife-edge diffraction calculations, allowing for ground reflections with a function $G(\bar{h}_{1,2})$ described in the earlier report (Rice et al., 1967). Criteria to determine when $G(\bar{h})$ should be used depend upon whether or not the radio ray has first Fresnel zone clearance above the terrain between an antenna and its horizon. For computer application this condition is approximated when the effective antenna height exceeds the maximum width of the first Fresnel zone. The computer method was therefore revised to calculate the knife-edge attenuation $A(v,0)$, using the parameters for the path, and the total attenuation as

$$A_{cd} = A(v,0) - G(\bar{h}_1) - G(\bar{h}_2) \quad dB, \tag{4}$$

where

$$\bar{h}_1 = 5.74\,(f^2/a_1)^{1/3}\; h_{e1},\quad a_1 = d_{L1}{}^2/2\,h_{e1},\quad \text{and} \tag{5a}$$

$$\bar{h}_2 = 5.74\,(f^2/a_2)^{1/3}\; h_{e2},\quad a_2 = d_{L2}{}^2/2\,h_{e2}. \tag{5b}$$

When $h_{e1,2} > 0.5\sqrt{\lambda\, d_{L1,2}}$ let $G(\bar{h}_{1,2}) = 0$; (6)

otherwise $G(\bar{h})$ is read from figure 7.2, volume 1 of Rice et al. (1967). Mathematical functions have been fitted to these curves for use in the computer method. In equations (4) through (6) all heights and distances are in km and the frequency is in MHz. The predicted value of basic transmission loss L_{bc} is then obtained by adding the free space loss L_{bf} to the calculated attenuation A_{cd}, as shown in equations (3a) and (3b).

A cumulative distribution of the differences between observed values and those calculated using this revised prediction method show excellent agreement.

Figures 55 and 56 show that both the earlier method and the computer method agree well with observed long-term median values for both two-horizon diffraction and forward scatter paths.

4. CONCLUSIONS

Several conclusions may be drawn from these comparisons of prediction methods with a large number of spot measurements and long-term recordings.

The "area" predictions, that do not require individual path profiles, define the medians of data as a function of distance either when the antenna sites are chosen at random, or the rules for site selection are clearly defined. The scatter of measured values about their median at each distance depends on site selection and the range of terrain irregularity in the group of paths considered. For homogeneous terrain